ISSN 1063-7826, Semiconductors, 2015, Vol. 49, No. 1, pp. 28–32. © Pleiades Publishing, Ltd., 2015.
Original Russian Text © D.A. Firsov, L.E. Vorobjev, V.Yu. Panevin, A.N. Sofronov, R.M. Balagula, I.S. Makhov, D.V. Kozlov, A.P. Vasil'ev, 2015, published in Fizika i Tekhnika Poluprovodnikov, 2015, Vol. 49, No. 1, pp. 30–34.

Terahertz Radiation Associated with the Impurity Electron Transition in Quantum Wells Upon Optical and Electrical Pumping

D. A. Firsov[a]^, L. E. Vorobjev[a], V. Yu. Panevin[a], A. N. Sofronov[a], R. M. Balagula[a], I. S. Makhov[a], D. V. Kozlov[b, c], and A. P. Vasil'ev[d]

[a] *St. Petersburg State Polytechnical University, St. Petersburg, 195251 Russia*
^e-mail: dmfir@rphf.spbstu.ru
[b] *Institute of Physics of Microstructures, Russian Academy of Sciences, Nizhni Novgorod, 607680 Russia*
[c] *Lobachevsky State University, Nizhni Novgorod, 603950 Russia*
[d] *Ioffe Physical–Technical Institute, Russian Academy of Sciences, St. Petersburg, 194021 Russia*

Submitted May 23, 2014; accepted for publication June 15, 2014

Abstract—Radiation in the terahertz (THz) spectral range from structures with GaAs/AlGaAs doped quantum wells is investigated under conditions of the interband optical excitation of electron–hole pairs in n-type structures and impurity breakdown in a longitudinal electric field in p-type structures. The emission spectra are obtained. Emission is observed at low temperatures and shown to be determined by optical transitions between impurity states and transitions between the band and impurity states. Upon optical interband pumping, the impurity states are depopulated due to the recombination of electron–hole pairs with the involvement of impurities, while, in an electric field, the impurity states are depopulated due to impact ionization.

DOI: 10.1134/S106378261501008X

1. INTRODUCTION

The development of efficient solid-state sources of terahertz (THz) spectral-range radiation (wavelength of 50–300 μm) is an important and urgent problem because the field of the potential application of such sources is extremely wide and includes information technologies, medicine, monitoring and safety systems, communication, and physical investigations of materials and structures [1]. A promising mechanism for THz-radiation emission can be based on the use of intracenter transitions of charge carriers in doped semiconductors and semiconductor nanostructures. The authors of [2] relate THz-radiation generation to the optical intracenter transition of holes in single-axis-deformed germanium in an electric field. Other examples of THz-radiation generation are known upon the transition of charge carriers between impurity states. This is a bulk-silicon laser with optical pumping [3] and emission upon the impact ionization of a neutral impurity by an electric field in bulk silicon [4]. The resonant states of an impurity can arise not only when applying external mechanical stress, as in [2], but also due to internal stresses in the structure formed upon the epitaxial growth of semiconductors with a different lattice constant. The THz emission from such structures in an electric field was investigated in [5].

In [1–5], THz radiation arose under nonequilibrium conditions upon the depopulation of impurity states by an electric field or intraband optical pumping. Recently, a different means of the depopulation of impurity states under conditions of the interband optical excitation of a doped semiconductor related to the recombination of nonequilibrium charge carriers through impurity states was proposed. The THz radiation associated with such a mechanism was revealed in bulk p-Ge and n-GaAs [6].

There are a few studies devoted to the investigation of THz radiation related to charge-carrier transitions between levels of impurity centers in semiconductor nanostructures with quantum wells (see, for example, [7], which describes THz radiation in a longitudinal electric field from structures with GaAs/AlGaAs quantum wells (QWs) with the involvement of impurity resonant states, which arose due to size quantization). Meanwhile, the characteristics of THz-radiation sources at impurity transitions in structures with QWs can be more attractive because of the possibility of controlling the impurity-ionization energy in such structures by varying the QW parameters.

In this publication, we present the results of the observation of spontaneous THz-range radiation in structures with doped GaAs/AlGaAs QWs. Two ways of exciting nonequilibrium charge carriers are used: electrical pumping and interband optical excitation. In the latter case, as well as in [6], the donor ground state is depopulated due to interband recombination with nonequilibrium holes, and the THz radiation

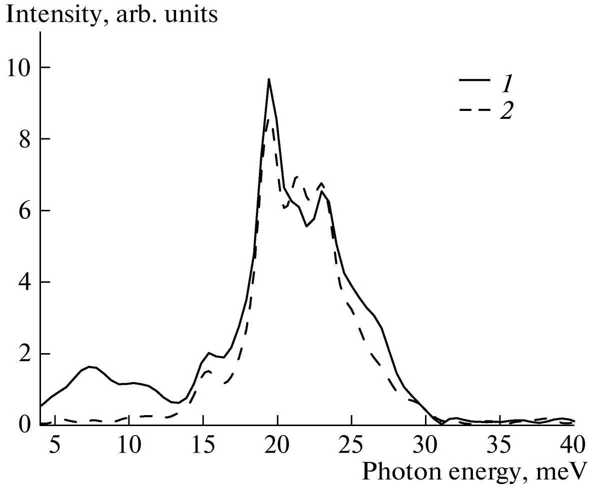

Fig. 1. Emission spectra of (*1*) a structure with *n*-type GaAs/AlGaAs QWs and (*2*) the substrate upon interband optical excitation at $T = 4.4$ K.

arises upon the transition of nonequilibrium electrons from the conduction band to donor levels.

2. THZ RADIATION UPON INTERBAND OPTICAL PUMPING

The samples for the investigations were grown by molecular-beam epitaxy on a GaAs semi-insulating substrate and contained a GaAs buffer layer 0.2 μm thick and 50 periods of $GaAs/Al_{0.3}Ga_{0.7}As$ QWs 30 nm in width. The QWs were separated by barriers 7 nm in width. Silicon doping was carried out in a layer 4 nm in width shifted with respect to the QW center by 6 nm. The concentration of donors amounted to 3×10^{10} cm^{-2}. The samples also contained a GaAs coating layer 20 nm thick doped with silicon to a level of 5×10^{17} cm^{-3}.

The measurements were carried out using a a Janis PTCM-4-7 closed-cycle cryostat which made it possible to maintain the temperature in the range of 4–320 K. Nonequilibrium charge carriers were excited by radiation modulated with a frequency of 87 Hz from a solid-state diode-pumped laser ($\lambda = 532$ nm, $P = 8$ mW) operating in the CW mode. With the help of an optical system, the pump radiation was focused on the sample surface at an angle of 45° to the growth axis of the structure. The THz radiation was directed from the sample surface along the growth axis through a poly(4-methylpentene-1) (PMP) window.

The photoluminescence spectra in the THz range were obtained using a Bruker Vertex 80v vacuum Fourier spectrometer. The entrance window of the spectrometer was made of polyethylene and the filter preventing the stimulating radiation from entering the spectrometer, of black polyethylene. The radiation was recorded by a silicon bolometer cooled to liquid-helium temperature. The measurements were carried out in the "step-scan" mode, and the bolometer signal was measured by an amplifier with an SR830 synchronous detector.

Under conditions of interband optical excitation, the generation of nonequilibrium electron–hole pairs takes place. At low temperature, the donors are neutral, and their ground state is occupied with electrons, which can recombine with nonequilibrium holes. The processes of the capture of nonequilibrium electrons from a quantum-confinement subband to charged-donor states can proceed in the emission mode and be accompanied with THz-radiation emission.

In Fig. 1, we show the experimentally observed THz-emission spectra from structures with QWs under conditions of interband optical pumping. In Fig. 1, we also show for comparison the spectrum of radiation from a sample without quantum-confinement layers (substrate spectrum). It should be noted that the real spectra can differ from those presented due to the spectral features of the optical system (beam splitters in the spectrometer, windows, and filters).

The experiment showed that a broad radiation line in the range of 15–30 meV is present in both spectra. This testifies that the radiation in this spectral range is not related to the presence of quantum-confinement layers in the structure under investigation. Since the stimulating radiation can penetrate into the substrate, the possible reasons for the occurrence of the line in the region of 15–30 meV can be related to processes in the substrate or to impurities adsorbed by the structure surface. Clarification of the nature of this radiation requires additional investigations.

The radiation line in the range of 4–13 meV is observed only in the sample with QWs. Optimization of the optical scheme for increasing the sensitivity of the installation in this spectral range enabled us to study this line in more detail. In Fig. 2, we show the emission spectra in the long-wavelength region measured at two temperatures.

The energies of the $e1 \longrightarrow 1s$ transition of electrons between the first quantum-confinement level and the impurity ground level and the $2p_{x,y} \longrightarrow 1s$ transition between the excited and impurity ground levels were calculated for this structure in [7] and amounted to 8.8 and 6.5 meV, respectively. These energies are shown in Fig. 2 by arrows. Satisfactory agreement between the calculated energies of electron transitions with the involvement of impurity levels and experimentally obtained spectra enables us to assume the presence of the above mechanism of THz-radiation emission.

With increasing temperature from 4.4 to 10 K, the radiation intensity decreases approximately 1.5 times; in this case, the emission spectrum remains invariable. A similar decrease in the radiation intensity from bulk semiconductors with temperature was revealed in [6], where a decrease in the probability of electron capture at a donor center with increasing temperature was pre-

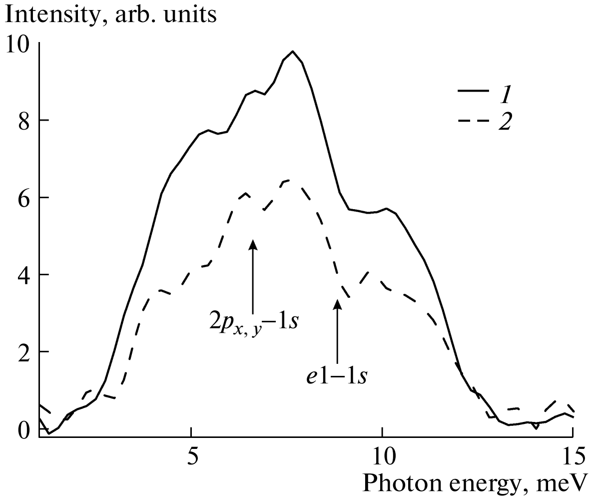

Fig. 2. Long-wavelength part of the emission spectrum for two lattice temperatures: (*1*) $T = 4.4$ K and (*2*) $T = 10$ K. The arrows show the calculated electron-transition energies.

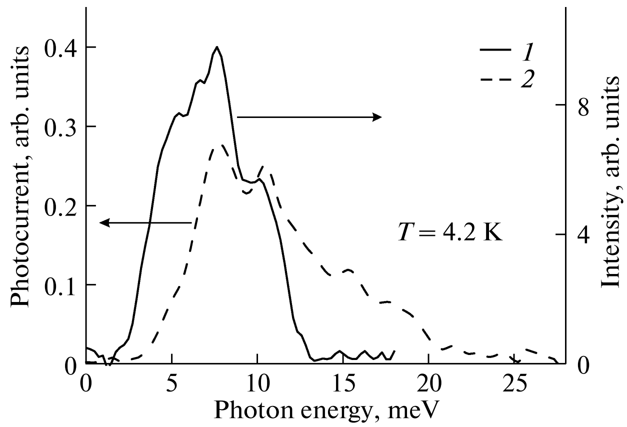

Fig. 3. Comparison of (*1*) the emission spectrum of radiation upon interband optical pumping and (*2*) the photoconductivity spectrum measured in the same structure [7].

sented as the possible cause of this. For detailed explanation of the temperature dependence, further investigations are necessary.

Additional confirmation of the impurity nature of the observed radiation is shown in Fig. 3 in which the impurity-photoconductivity spectrum of this structure taken from [7] is presented along with the emission spectrum.

The spectra shown in Fig. 3 are similar; however, they differ in the long- and short-wavelength portions. The short-wavelength tail of the photoconductivity spectrum, which is not presented in the emission spectrum, can be related to electron transitions from an impurity level to the states of the quantum-confinement subband with a large value of the wave vector. At the same time, the long-wavelength part of the emission spectrum can be determined by the radiative electron transition from the first subband to the impurity excited states.

3. THZ RADIATION UPON EXCITATION BY A LONGITUDINAL ELECTRIC FIELD

In the second part of the study, we investigated the radiation from doped structures with GaAs/AlGaAs QWs under conditions of impurity breakdown in a longitudinal electric field. Previously, we observed THz radiation in the electric field from the *n*-type structures with QWs; this radiation was related to the transition of electrons excited by the electric field between the impurity resonant and localized states [7]. In this study, we used *p*-type structures, which is related to the high ionization energy for the Be acceptor impurity. The high ionization energy amounted to 46 meV in our structures and exceeded the optical-phonon energy. Under such conditions, the capture of nonequilibrium holes from the valence band to the Be-impurity ground level with optical-phonon emission is impossible. The capture of nonequilibrium holes from the band to acceptor excited states with optical-phonon emission is possible, which can favor an increase in intensity of the THz-radiation related to the intracenter transitions of holes to the impurity ground level.

We used structures grown by molecular-beam epitaxy on a semi-insulating GaAs substrate containing a GaAs buffer layer 0.2 mm thick and 200 periods of GaAs/$Al_{0.4}Ga_{0.6}As$ QWs 3.8 nm in width. The QWs were separated by barriers 7 nm in width. Be doping was carried out in the central part of the QW in a layer 0.8 nm in width. The concentration of acceptors amounted to 3.2×10^{11} cm^{-2}. The samples also contained a GaAs coating layer 20 nm thick doped with silicon to a level of 5×10^{17} cm^{-3}. The contacts to the samples were represented by two narrow parallel indium strips deposited onto the structure surface and annealed in a nitrogen atmosphere at a temperature of 450°C; they provided the possibility of the application of an electric field in the structure plane to all layers of QWs.

In Fig. 4, we show the *I*–*V* characteristic and the electric-field dependence of the integral radiation intensity measured at a temperature of 4.2 K in the mode of single electric-field pulses 2 μs long. The sample and Ge(Ga) photodetector were located in a transport Dewar vessel for liquid helium. The radiation appears in electric fields exceeding the impurity-breakdown field, which is approximately 1000 V/cm.

The emission spectra were studied using the technique described mainly in the previous section. The difference consisted in the method of the excitation of nonequilibrium holes, i.e., impurity breakdown in a longitudinal field was used. In order to avoid Joule heating of the sample, the electric field was applied in the form of sequences of four pulses 20 μs long.

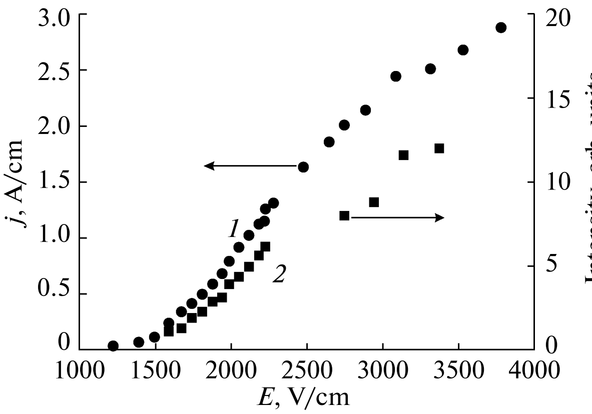

Fig. 4. (*1*) *I–V* characteristic and (*2*) the integral intensity of the THz radiation measured at $T = 4.2$ K in the structures with *p*-type GaAs/AlGaAs QWs.

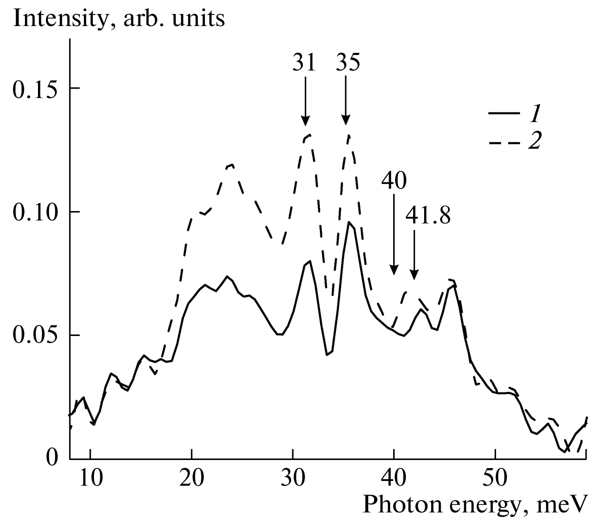

Fig. 5. Emission spectra of a structure with *p*-type GaAs/AlGaAs QWs in a longitudinal electric field of (*1*) 560 V/cm and (*2*) 680 V/cm. The temperature is $T =$ 15 K. The numbers near the arrows designate the calculated intracenter-transition energies (in meV).

The distance between the pulses amounted to 1.5 ms, and the series repetition frequency was 87 Hz.

In Fig. 5, we show the experimental emission spectra measured at $T = 15$ K for various intensities of the longitudinal electric field. The breakdown electric-field strength at this temperature determined from the *I–V* characteristic amounts to approximately 400 V/cm.

To clarify the nature of the radiation under observation, we calculated the energies of the Be-impurity levels in the structure under investigation. The calculations were carried out in the effective-mass approximation. The Hamiltonian of equations for wave-function envelopes involves the Luttinger Hamiltonian restricting the QW potential, the Coulomb potential of acceptor point charge, and the potential of the central cell describing the chemical shift. We used the axial approximation; in this case, the terms proportional to $(\gamma_2 - \gamma_3)$ (γ_2, γ_3, are the Luttinger parameters) were omitted in nondiagonal elements. In the axial approximation, the projection of the total momentum to the QW normal is retained, and the acceptor spectrum proves to be twice degenerate in sign of this projection. The acceptor wave function was expanded with respect to the basis of the envelope wave functions $v_n^s(\mathbf{k}, z)e^{i\mathbf{k}\boldsymbol{\rho}}$ of free holes in the QW, which are the eigenfunctions of the Hamiltonian in the absence of the impurity potential. (Here, n is the number of the quantum-confinement subband, $\boldsymbol{\rho}$ is the radius vector in the QW plane, $\mathbf{k}$ is the hole wave number, and $s =$ 1, ..., 4 is the number of the component of the hole vector function). Substituting this expansion in the effective-mass equation, we obtain the integral equation for the expansion coefficients. Further, the integral can be replaced by a discrete sum over k; in this case, the step in k should be chosen to be shorter than the reciprocal Bohr radius in order that the integrand varies only slightly per step. Summation can be interrupted for values of k greatly exceeding the reciprocal Bohr radius. Thus, the problem is reduced to diagonalization of the finite-dimensional Hermit matrix.

To calculate the value of the chemical bias for the acceptor boron impurity located at an arbitrary point of the heterostructure, we used, similar to [8], the model potential, which is significant in the vicinity of the acceptor ion:

$$\Delta V = \left[\frac{1}{\varepsilon} - \frac{1}{\varepsilon_0}\right]\frac{e^{-r/a}}{r},$$

where $a = 5.65$ Å (GaAs lattice constant); $\varepsilon_0 = 13.6$ is the GaAs permittivity; and $1 < \varepsilon < 11.4$ is the effective permittivity, which is the fitting parameter chosen from best agreement of the calculation results with available experimental data for the energy of the ground state of the Be impurity in bulk GaAs. The value of this parameter was found to be $\varepsilon = 8.5$.

The scheme of the obtained energy levels for acceptors is shown in Fig. 6. Wide lines correspond to larger values of the optical matrix element.

In Fig. 5, the arrows show the photon energies corresponding to the allowed transitions of holes with the involvement of impurity states. The position of experimental emission spectra is in satisfactory agreement with the calculated energies of impurity transitions. In this case, the experimental spectrum extends into the region of low photon energies of 20–28 meV. The corresponding radiation can be associated with the transitions of hot heavy holes from the *hh*1 subband to excited acceptor states. The radiation intensity into the photon-energy region exceeding 40 meV is low despite the large oscillator strength calculated for transitions amounting to 40 and 41.8 meV. This can be

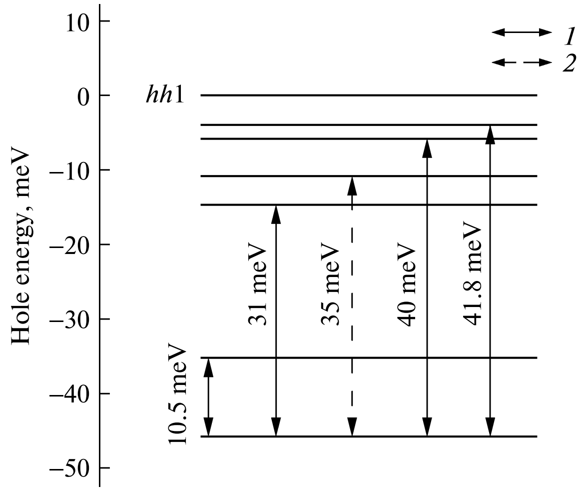

Fig. 6. Calculated acceptor-energy levels associated with the first heavy-hole subband *hh*1 in a structure with GaAs/AlGaAs QWs. The 31–41.8-meV arrows indicate the allowed hole optical transitions for (*1*) *s* polarization and (*2*) *z* polarization of the light. Transitions of 40 and 41.8 meV correspond to large values of the optical matrix element.

attributed to the closeness of the corresponding photon energies to the energy of the transverse optical phonon in the AlAs sublattice.

4. CONCLUSIONS

Thus, we showed in the study that it is possible to observe THz-range emission in structures with GaAs/AlGaAs quantum wells related to the transition of charge carriers to the impurity states. Two means of depopulation of the impurity ground state are shown: (i) interband optical excitation resulting in the recombination of electron–hole pairs with the involvement of impurity states and (ii) impurity breakdown in a longitudinal electric field.

ACKNOWLEDGMENTS

This study was supported by the Russian Foundation for Basic Research (project nos. 12-02-01155 and 14-02-90444), by the Ministry of Education and Sciences of the Russian Federation (the state quota), and by the German–Russian Program of the Federal Ministry of Education and Research (BMBF).

REFERENCES

1. M. Tonouchi, Nature Photon. **1**, 97 (2007).
2. Yu. P. Gousev, I. V. Altukhov, K. A. Korolev, V. P. Sinis, M. S. Kagan, E. E. Haller, M. A. Odnoblyudov, I. N. Yassievich, and K.-A. Chao, Appl. Phys. Lett. **75**, 757 (1999).
3. S. G. Pavlov, R. Kh. Zhukavin, E. E. Orlova, V. N. Shastin, A. V. Kirsanov, H.-W. Hübers, K. Auen, and H. Riemann, Phys. Rev. Lett. **84**, 5220 (2000).
4. P.-C. Lv, R. T. Troeger, T. N. Adam, S. Kim, J. Kolodzey, I. N. Yassievich, M. A. Odnoblyudov, and M. S. Kagan, Appl. Phys. Lett. **85**, 22 (2004).
5. V. A. Shalygin, L. E. Vorobjev, D. A. Firsov, V. Yu. Panevin, A. N. Sofronov, A. V. Andrianov, A. O. Zakhar'in, A. Yu. Egorov, A. G. Gladyshev, O. V. Bondarenko, V. M. Ustinov, N. N. Zinov'ev, and D. V. Kozlov, Appl. Phys. Lett. **90**, 161128 (2007).
6. A. V. Andrianov, A. O. Zakhar'in, Yu. L. Ivanov, and M. S. Kipa, JETP Lett. **91**, 96 (2010).
7. D. A. Firsov, V. A. Shalygin, V. Yu. Panevin, G. A. Melentyev, A. N. Sofronov, L. E. Vorobjev, A. V. Andrianov, A. O. Zakhar'in, V. S. Mikhrin, A. P. Vasil'ev, A. E. Zhukov, L. V. Gavrilenko, V. I. Gavrilenko, A. V. Antonov, and V. Ya. Aleshkin, Semiconductors **44**, 1394 (2010).
8. N. O. Lipary, A. Baldereschi, and M. L. W. Thewalt, Solid State Commun. **33**, 277 (1980).

Translated by V. Bukhanov